

Investigation into Self-calibration Methods for the Vexcel UltraCam D Digital Aerial Camera

K. S. Qtaishat¹⁾ and M. J. Smith

¹⁾ Civil and Environment Engineering Department, Mu'tah, University, Mu'tah, Al-Karak, Jordan, 61710
khaldoun_q@hotmail.com

ABSTRACT

This paper provides an investigation into the camera calibration of a Vexcel UltraCam D digital aerial camera which was undertaken as part of the EuroSDR Digital Camera Calibration project. This paper will present results from two flights flown over a test site at Fredrikstad-Norway using established camera calibration techniques. Furthermore, it proposes an alternative approach.

The "new" multi cone digital camera systems are geometrically complex. The image used for photogrammetric analysis is made up of a number of images produced by a cluster of camera cones and possibly various groups of CCD arrays. This produces a resultant image which is not just based on traditional single lens/focal plane camera geometries, but depends on the joining of images from multiple lens (different perspectives), handling groups of focal planes and the matching of overlapping image areas. Some of the requirements from camera calibration such as stability can only be determined through long-term experience/research and some can be determined through investigation and short-term research such as the calibration parameters. The methodology used in this research for assessing the camera calibration is based on self-calibration using the Collinearity Equations. The analysis was undertaken in order to try to identify any systematic patterns in the resulting image residuals.

By identifying and quantifying the systematic residuals, a new calibration method is proposed that re-computes the bundle adjustment based on the analysis of the systematic residual patterns. Only very small systematic patterns could be visually identified in small areas of the images. The existing self-calibration methods and the new approach have made a small improvement on the results. The new calibration approach for the low flight has been particularly beneficial in improving the RMSE in Z and reducing image residuals. However, the method was less successful at improving the high flown results. This approach has shown that it has potential but needs further investigation to fully assess its capabilities.

KEYWORDS: Digital cameras, Aerial triangulation, Camera calibration, Digital images.

INTRODUCTION

Camera Calibration

There are now many different digital sensor systems available for photogrammetry, remote sensing and

digital image analysis. Cramer (2005) provides a summary of the systems available in 2005 and these include single and multi-cone/lens systems as well as high resolution push broom scanners. Before any imagery can be used for high precision measurement purposes in photogrammetry, there is a need to determine the geometric model of the sensing system. In

Accepted for Publication on 15/4/2010.

the case of frame cameras, there is a need to establish the sensor model and determine the relationship of this model in comparison to the standard normally (and traditionally) used in photogrammetry which is perspective geometry. The process of measuring the relationship of a "real" frame camera geometry in comparison to perspective geometry is known as camera calibration. Camera calibration is normally undertaken by the manufacturer before supplying a camera for photogrammetry, then periodically and when necessary during the life of the camera.

The "new" multi cone digital camera systems are geometrically complex systems. The image used for photogrammetric analysis is made up of a number of images produced by a cluster of camera cones and possibly various groups of CCD arrays. This produces a resultant image which is not just based on traditional single lens/focal plane camera geometries, but depends on the joining of images from multiple lens (different perspectives), groups of focal planes and the matching of overlapping image areas. For optimal use of this imagery, there is a need to:

1. Understand this complex geometric model;
2. Undertake a calibration of the "real" camera;
3. Analyse the relationship between the calibrated camera geometry and perspective geometry;
4. Establish whether existing calibration procedures are adequate;
5. Possibly establish new procedures;
6. Establish how long a camera calibration lasts before periodic recalibration is required.

Some of these requirements can only be determined through long-term experience/research and some can be determined through investigation and short-term research. This paper provides an investigation into the camera calibration of a Vexcel UltraCam D aerial camera based on results achieved from two flights flown over a test site over Fredrikstad-Norway as part of the EuroSDR Digital Camera Calibration project.

Objectives

The main objective of this research was to

investigate the calibration of a Vexcel UltraCam D digital aerial camera. This will involve investigating the following objectives:

1. Understanding the geometry of the UltraCam D;
2. Establishing whether existing camera calibration techniques are suitable;
3. Possibly proposing an alternative camera calibration approach.

Methodology

The EuroSDR project provided a data set consisting of two UltraCam D sorties taken at different altitudes over a targeted (pre-marked) test site in Norway. The available data and facilities influence the methodology that can be adopted. A brief description of the camera geometry is given in the "TECHNOLOGY"- section in this study and this provides the guide for the detailed issues to be investigated.

The methods used for the investigation are as follows:

1. The geometry of the camera is obtained from a literature review (objective 1) and this is reported in the "TECHNOLOGY"- section.
2. The proposed method of camera calibration will be based on the self-calibration technique using the Collinearity Equations (objective 2 and objective 3) and this is reported in the "TRIALS AND ANALYSIS"- section.

Variables in the self-calibration technique to be investigated are as follows:

1. Number of tie points used in joining the images; this was investigated on the benchmark result only, making a reasonable assumption that this would be typical of all other triangulations.
2. Number of control points and number of check points; this was investigated on the benchmark result only, making a reasonable assumption that this would be typical of all other triangulations.
3. Calibration model used;
 - As a camera calibration has already been performed by Vexcel and applied by IFMS, a triangulation will be performed without a

calibration model (additional parameters) which can be used as a "benchmark result" against which other results can be compared.

- The "best" result from existing traditional models will be identified based on image residuals and RMSE of ground and check points. In theory, the existing traditional self-calibration models have been based on knowledge and experience of single cone frame camera geometries and environmental effects. As such it might be reasonable to expect only limited benefit from using these models with a multi-lens system. The mathematical functional model for the self-calibration bundle adjustment is based on the collinearity condition which is implied in the perspective transformation between the image pixel coordinate system or other image coordinate measurement system to the image space coordinate. Using a 2D affine transformation, the relationship between the pixel coordinate system and the image space coordinate system is defined. The self-calibrating methods use additional parameters in the triangulation process to eliminate the systematic errors. The following 2D affine transformation equations after setting the following camera calibration parameters: f , dx , dy , a_1 , a_2 , a_3 , a_4 , a_5 , a_6 , a_7 , a_8 , a_9 , a_{10} , a_{11} and a_{12} :

$$x = X + dx + a_1X + a_2Y + a_3XY + a_4X^2 + a_7r + a_8r^3 + a_9r^5$$

$$y = Y + dy + a_5XY + a_6Y^2 + a_7r + a_8r^3 + a_9r^5$$

where:

x and y are the image coordinates associated with the calibrated fiducial marks.

X and Y are the pixel coordinates of the measured fiducial marks.

dx and dy represent the principal point position.

a_7 , a_8 and a_9 are polynomial coefficients for radial lens distortions.

a_1 , a_2 , a_3 , a_4 , a_5 and a_6 represent the six affinity transformation.

r is the radial distance from the principal point.

- As the geometry of the UltraCam D is different from the traditional single cone/CCD camera, an

analysis will be undertaken in order to try to identify if there are any systematic patterns in the image residuals (objective 3). This will enable new calibration procedures (objective 3) to be considered.

Two calibration approaches can be identified to deal with multi-lens cameras:

- a. Based on an appropriate choice of additional parameters during the bundle adjustment;
- b. By identification and quantification of systematic image residual patterns followed by their application to image coordinates and re-computation of the bundle adjustment.

The purists might argue that approach "a" is the "best" approach with some justification, but approach "b" does have some advantages:

- a. it can be applied to any multi-lens camera system with little or no change to the bundle adjustment computation;
- b. it only requires some post-processing software to analyse the residuals and some pre-computation software to apply the corrections, not a change to existing aerial triangulation software;
- c. it can consider systematic effects on image coordinates from any sources and not those just depending on modeling optical geometry.

Approach "b" will be investigated and for convenience it will be identified as the "IESSG approach". In this approach, image residuals from all images will be analysed in a sub-area of the image and a residual representing the sub-area will be used to show any systematic effect. For example, this could involve dividing the image into 25x25 subareas giving 8x8 numbers of sub-areas/points per CCD. Investigating residual plots of various numbers of subdivisions from one residual per CCD up to a high density of points per CCD, the 25x25 division seems to give a reasonably detailed distribution of residuals. The 25x25 division also appeared to give a reasonable indication of any systematic patterns and therefore image coordinate correction, without swamping with too much detail and random error which was found with some other subdivisions.



Figure (1): Multiple lens cones; 4 panchromatic across the centre and 4 larger colour cones (Copyright Simmons Aerofilms, Ltd.) (Smith et al., 2005)

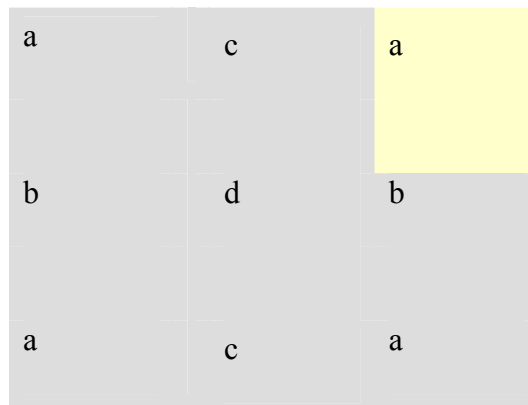


Figure (2): Schematic of the 9 sub-images making up the panchromatic image with one image highlighted

Test Site and Data Provided by EuroSDR Project

Data Provider: IFMS-Pasewalk / Germany

Test Site: Fredrikstad-Norway

Mission Flight: 16 September 2004

Image used: Panchromatic image

In-flight GPS/IMU: None used

High flight:	Flying height:	3800m	
	Number of images:	29	
	Number of control points available:	14	
Low flight:	Flying height:	1900m	
	Number of images:	132	
	Number of control points available:	17	
Overlap:	80% forward and 60% lateral overlap		

Standard error of ground control points = $\pm 0.050\text{m}$.
Check ground points were provided but at a lower quality than the control points so they are of limited value in this analysis.

Facilities Available for Digital Image Processing and Camera Calibration

- LPS -used for image point observations and automatic tie point measurement.
- ORIMA - used for aerial triangulation computation with and without self-calibration.
- In-house analysis tools - used to analyse results.

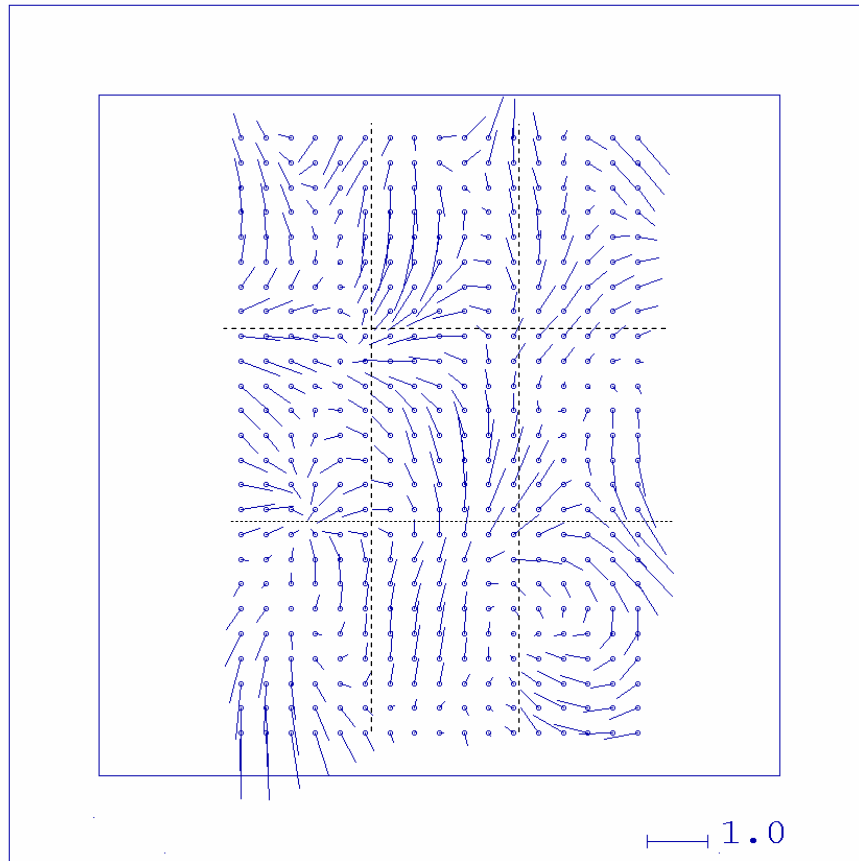


Figure (3): Mean image residuals in 25x25 sub-areas, results of AT without any calibration model (high flown) (coordinates in pixels, partitioning shows approx. boundaries of the CCD arrays)

Presentation of Results

The results will be presented in two ways:

1. In tables of RMSE on control, check and image points. The EuroSDR project requested that the coordinates of a number of prescribed check points are included in the computation enabling a check point analysis to be performed. It has not been possible to include a meaningful analysis of these check points as their coordinates have not been provided to a suitable accuracy. So some selected points from the control list have been used as check points.
2. In graphical form showing the mean image residuals computed from all the image measurements, from all the images within a small sub-area of the image. It is important to note that

the scale of the residuals varies between figures/plots, see the scale arrow in the bottom right hand corner of each figure.

TECHNOLOGY

Camera and Image Geometry (objective 1)

The Vexcel UltraCam D digital aerial camera consists of 8 lens cones as shown in Figure 1 (Smith et al., 2005; Kruck, 2006; Gruber and Ladstädler, 2006). The 4 lens cones in a line through the centre of the cone cluster are used to capture the panchromatic image which is made up of 9 overlapping sub-images to create a composite image as shown schematically in Figure 2. The sub-images have been given a letter to show which images were captured by the same lens cone.

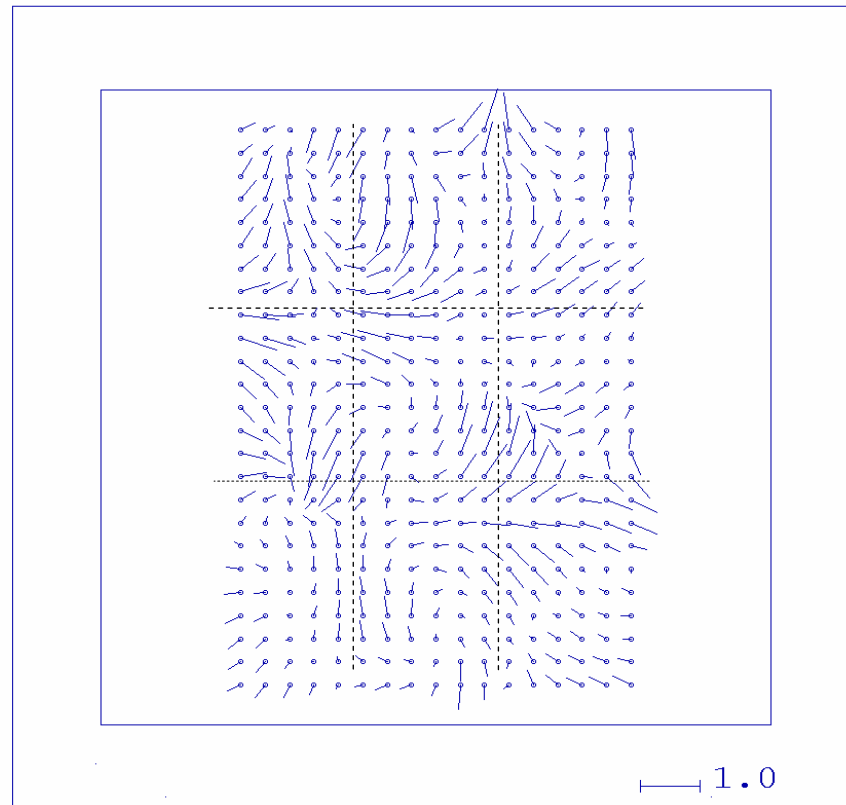


Figure (4): Mean image residuals in 25x25 sub-areas, results of AT with self-calibration model (high flown) (coordinates in pixels, partitioning shows approx. boundaries of the CCD arrays)

Points to note for analysis of the suitability of self-calibration techniques:

1. Self-calibration techniques have not traditionally calibrated multi-lens cameras.
2. Self-calibration techniques could take into consideration in-flight effects:
 - a. Overall camera/image parameters for the composite image (see Figure 2);
 - b. Image flatness;
 - c. Environmental effects:
 - i. Atmospheric refraction effects;
 - ii. Thermal effects on the camera;
 - iii. Atmospheric pressure effects on the camera.
 - d. Systematic effects of margining/matching of the sub-images together.

TRIALS AND ANALYSIS

Results and Discussion-General

Quality of the Images: It should be noted that the image observation was affected by the radiometric image quality in both the high flight and the low flight. This made the observation of some of the control points difficult and probably had an impact on the quality of automatic tie point generation. The histogram was adjusted appropriately for each separate image observation. The standard error used for the image observations was the σ_0 value from a preliminary run of the aerial triangulation for a particular block being analysed, typically 1-2 μm .

Number of Tie Points Used in Joining the Images: 900 tie points (132 images) were used in the low flight and 2300 tie points (29 images) were used in the high flight. The robust blunder detection algorithm was applied in LPS.

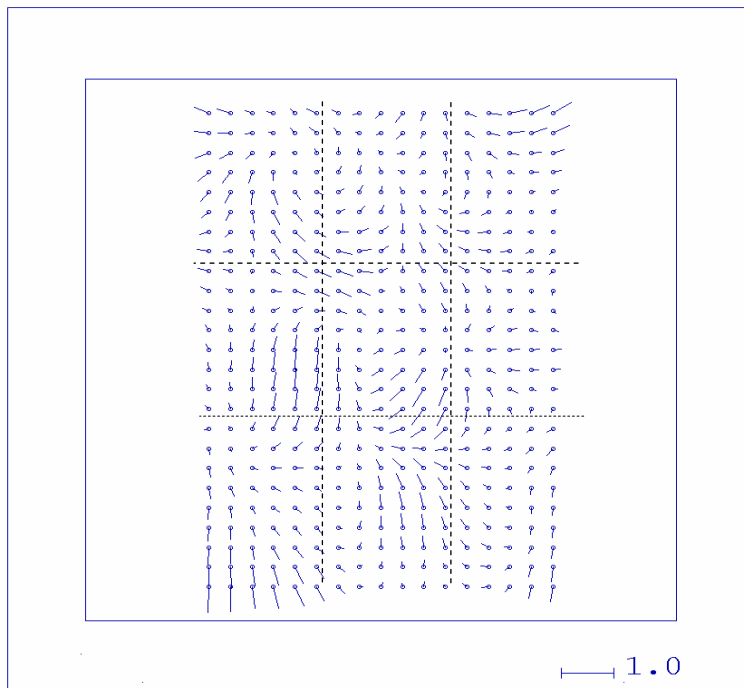


Figure (5): Mean image residuals in 25x25 sub-areas, results of AT with IESSG approach (high flown) coordinates in pixels, partitioning shows approx. boundaries of the CCD arrays)

Table (1): Summary of high flight results

Calibration Model	Ground control points RMSE (m) of residuals			Ground check points RMSE (m) of residuals			Image coordinates RMSE (μm) of residuals		Image coordinates RMSE (Pixel) of residuals	
	X	Y	Z	X	Y	Z	x	y	x	y
No	0.048	0.026	0.031	0.108	0.102	0.278	1.690	1.820	0.188	0.202
Self Calibration	0.042	0.024	0.020	0.120	0.104	0.248	1.590	1.730	0.177	0.192
residuals from IESSG	0.038	0.022	0.018	0.129	0.098	0.280	1.530	1.620	0.170	0.180

Table (2): Summary of low flight results

Calibration Model	Ground control points RMSE (m) of residuals			Ground check points RMSE (m) of residuals			Image coordinates RMSE (μm) of residuals		Image coordinates RMSE (Pixel) of residuals	
	X	Y	Z	X	Y	Z	x	y	x	y
No	0.054	0.034	0.042	0.042	0.038	0.186	1.320	1.310	0.147	0.146
Self Calibration	0.052	0.037	0.033	0.031	0.032	0.093	1.240	1.200	0.138	0.133
residuals from IESSG	0.055	0.038	0.028	0.037	0.037	0.038	1.060	1.000	0.118	0.111

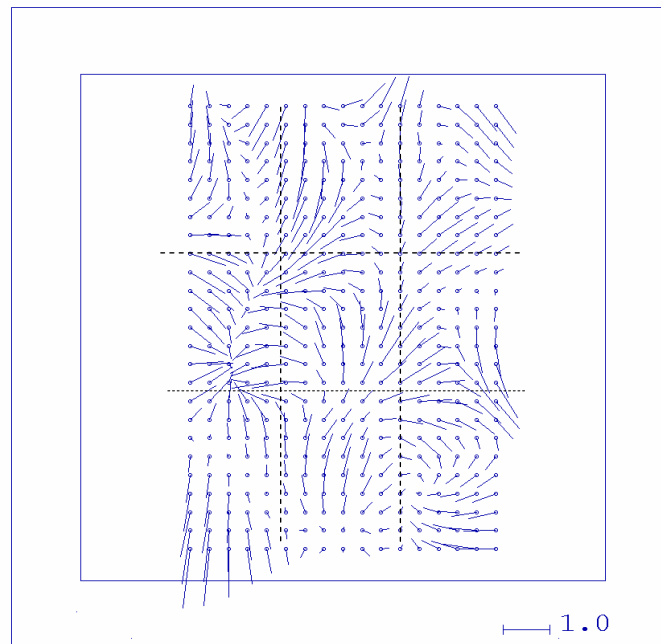


Figure (6): Mean image residuals in 25x25 sub-areas, results of AT without calibration model (low flow)
(coordinates in pixels, partitioning shows approx. boundaries of the CCD arrays)

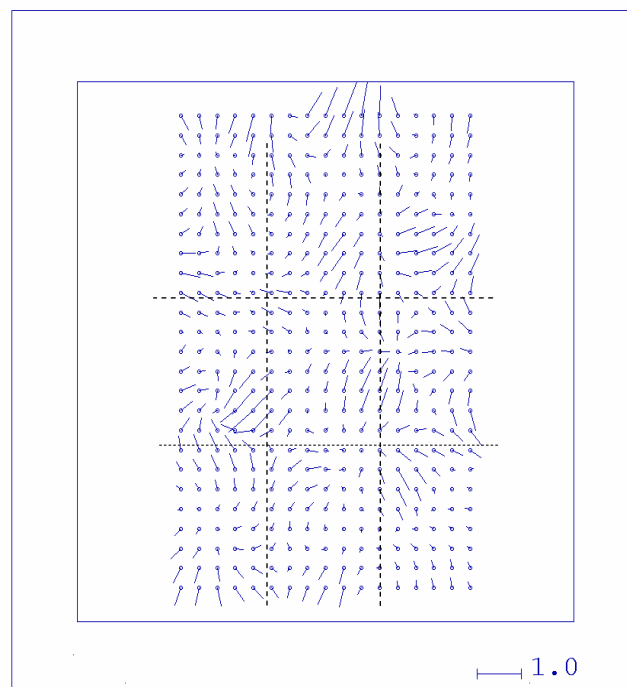


Figure (7): Mean image residuals in 25x25 sub-areas, results of AT with calibration model (low flow)
(coordinates in pixels, partitioning shows approx. boundaries of the CCD arrays)

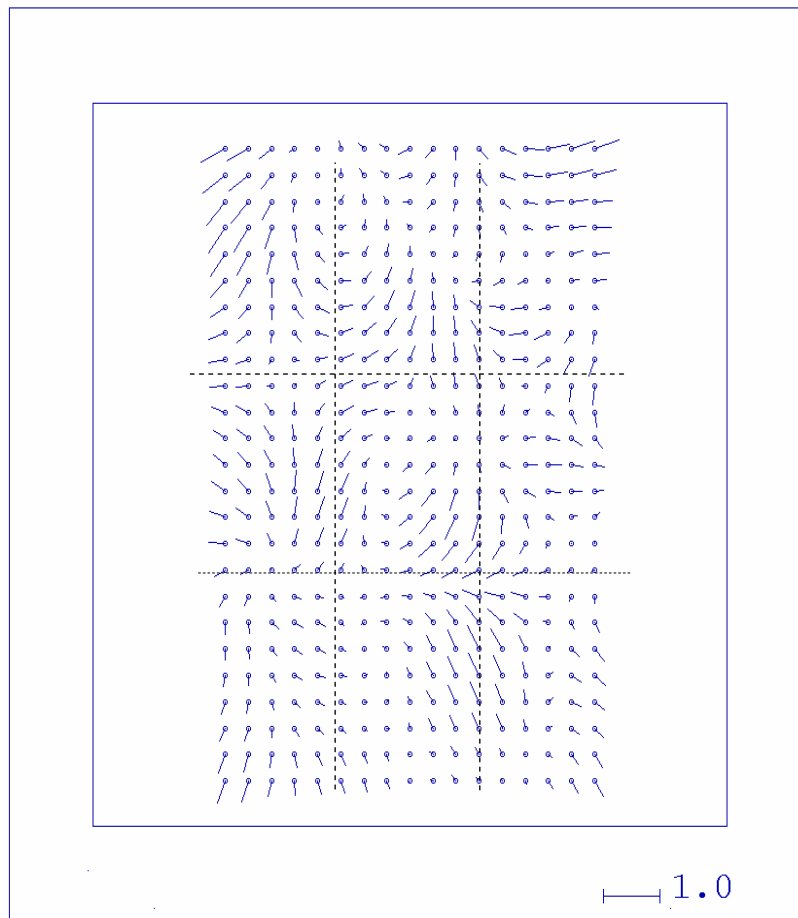


Figure (8): Mean image residuals in 25x25 sub-areas, results of AT with IESSG calibration model (low flown) (coordinates in pixels, partitioning shows approx. boundaries of the CCD arrays)

Number of Control Points and Number of Check

Points: For the low flight, it was decided to use 14 ground control points plus 3 ground control points as check points. For the high flight, it was decided to use 11 ground control points plus 3 ground control points as check points.

Results and Discussion-High Flight (3800m)

No Calibration Model-Benchmark Result: As a camera calibration has already been performed by Vexcel and results applied by IFMS, a triangulation was performed without a calibration model which can be used as a "benchmark result" against which other results

can be compared.

Figure 3 indicates the image residuals for the results presented in Table 1. On visual inspection of Figure 3, there is no overall identifiable systematic patterns in the whole image. There are small areas where systematic patterns can be identified, some showing a relationship to the CCDs (for example see bottom left corner) but it should be noted that in general the image residuals over the whole image are very small. As these residuals could come from a variety of sources and this only results from one block, these patterns may not be due to just uncorrected systematic characteristics of camera/image geometry. This raises the question: "Is

this pattern of residuals repeatable between blocks of images?"

The "Best" Result from Existing Self-Calibration Models: A number of self calibration models were tested from Leica LPS and ORIMA software to assess the most suitable one for this type of imagery. The results presented here come from ORIMA and are considered the "best" result from existing self-calibration models based on the assessment of image residuals and RMSE of ground and check points. The parameters of the self-calibration model are as follows:

c = principal distance;

x_0, y_0 = principal point position;

a_1, a_2, a_3 = polynomial coefficients for radial lens distortions.

The results in Table 1 show a very small improvement (except check point RMSE in X and Y) compared to the benchmark values. Figure 4 shows a similar pattern of the image residuals to those in Figure 3.

Analysis of Aerial Triangulation Image Residuals- IESSG Approach: Applying the results shown in Figure 3 to the measured image coordinates as described earlier in this study gives the "IESSG" results in Table 1. Figure 5 shows the mean image residuals of the observations for the sub-areas in the image using ORIMA without any additional parameters being used. The solution appears to have reduced some of the residual pattern although the top right hand corner seems to still have some relatively large residuals.

Summary of High Flight Results: Table 1 shows the results where the ground control RMSE values are significantly better than the ground control check point RMSE values. The ground control RMSE values are influenced by the standard errors of the image coordinates and the ground control. The standard error of $\pm 0.05\text{m}$ for the ground control was provided, and the standard error used for the image observations was the σ_0 value from a preliminary run of the aerial triangulation for a particular block being analysed, typically 1-2 μm . Table 1 also shows, in general, that a very slight improvement has been obtained from the self-calibration model. The self-calibration model is

probably correcting for some environmental effects. The IESSG approach has slightly improved the RMSE of the image residuals, causing a minimal improvement on the ground control RMSE values, but has made no real improvement on the check point RMSE values (considering RMSE in X and Z).

The Z RMSE for the check points in all three cases is dominated by one large Z residual which is greater than -0.3m in each case. If this value is removed, the RMSE of the remaining points is around the 0.1m level.

Results and Discussion-Low Flight (1900m)

A similar process used for analysing the high flown images has been used to assess the low flown images except for the IESSG approach where the high flown residual corrections have been used in the low flown computation. This correction was used because an ideal scenario would be to compute the residual corrections from a block of triangulation and then assuming this was a systematic pattern for all images. This would be applied until a new correction was computed. It is important to note that the results from the aerial triangulation in ORIMA were obtained without using the cross strip available for the low flight.

No Calibration Model-Benchmark Result: It is interesting to note that the image coordinate RMSE values are smaller than for the high flight, indicating a better quality of measurement and/or image quality. The RMSE values of the ground check points are good in X and Y, but the Z value for the check points is a little large compared with the ground control Z value. This value is dominated, like in the high flight, by one residual greater than 0.3. Figure 6 shows the image residuals for the results presented in Table 2. Visual inspection with Figure 3 shows that there are some similarities, see top and bottom left corners.

The "Best" Result from Existing Self-Calibration: A number of self-calibration models were tested from Leica LPS and ORIMA software to assess the most suitable one for this type of imagery. The results presented here come from ORIMA and are considered the "best" result from existing self-

calibration models based on the image residuals and RMSE of ground and check points. The parameters of the self-calibration model are as follows:

c = principal distance;

x₀, y₀ = principal point position;

a₁, a₂, a₃ = polynomial coefficients for radial lens distortions.

Figure 7 indicates the image residuals for the results presented in Table 2. There is a similar pattern of residuals to those shown in Figure 6 and to a lesser extent Figure 4.

Analysis of Aerial Triangulation Image Residuals

- IESSG Approach: In this trial, the image coordinate corrections that have been applied are the values computed from the high-flown block. Figure 8 indicates the image residuals for the results presented in Table 2. It appears, from visual inspection, that some of the patterns have been reduced.

Summary of Low Flight Results: Table 2 shows again small RMSE values for the ground control points as identified in the high flown trials. It also shows a small improvement in applying a traditional single lens self-calibration model technique. The interesting improvement comes from applying the IESSG approach which has reduced relatively significantly the x and y image residuals and the Z RMSE values for the check points compared to their bench mark values. This is using the residual corrections from the high flown

block. The relatively large Z RMSE for the check points in the "no calibration" computation is dominated, like in the high flight, by one residual greater than 0.3.

CONCLUSIONS

Only very small systematic patterns could be visually identified in small areas of the image. The existing self-calibration methods and the IESSG approach have made a small improvement on the results. The IESSG calibration approach for the low flight has been particularly beneficial in improving the RMSE in Z and reducing image residuals. However, the method was relatively less successful at improving the high flown results.

More tests and trials are required with a number of blocks to fully understand the residual patterns that are being produced not only within the images of a block but also between blocks.

The IESSG approach has shown that it has potential but needs further investigation to fully assess its capabilities. It is a little surprising that this approach did not make more improvement with the high flown block, which was used to compute the correction, as it did with the low flown block. Issues such as optimum subdivision of the image would also need to form part of this investigation.

A similar trial and analysis is being undertaken using both the high and the low flown flights together.

REFERENCES

- Cramer, M. 2005. Digital Airborne Cameras-Status and Future. ISPRS Hannover workshop on high resolution earth imaging for geospatial information, *Proceedings*, Volume XXXVI, Part I/W3, ISSN No. 1682-1777.
- Gruber, M. and Ladstädler, R. 2006. Geometric issues of the digital large format aerial camera UltraCam D. International Calibration and Orientation Workshop, EuroCOW 2006. January 2006, Castelldefels, Spain. EuroSDR Commission I and ISPRS Working Group 1/3.
- Kruck, E. 2006. Simultaneous calibration of digital aerial survey cameras. International Calibration and Orientation Workshop, EuroCOW 2006. January 2006, Castelldefels, Spain. EuroSDR Commission I and ISPRS Working Group 1/3.
- Smith, M. J., Qtaishat, K., Park, D. and Jamieson, A. 2005. Initial results from the Vexcel UltraCam D digital aerial camera. ISPRS Hannover workshop on high resolution earth imaging for geospatial information, *Proceedings*, Volume XXXVI, Part I/W3, ISSN No. 1682-1777.